

JGR Space Physics

RESEARCH ARTICLE

10.1029/2019JA026744

Key Points:

- New techniques are proposed for obtaining electron density profiles from incomplete radio-occultation data
- AVHIRO technique generates accuracies at 7% relative error, with computing time of 20 min in an Intel i7 standard PC
- SEEIRO generates accuracies at 11% relative error, about 60 times faster than AVHIRO, suitable for real-time applications

Correspondence to:

M. Hernández-Pajares,
manuel.hernandez@upc.edu

Citation:

Lyu, H., Hernández-Pajares, M., Monte-Moreno, E., & Cardellach, E. (2019). Electron density retrieval from truncated radio occultation GNSS data. *Journal of Geophysical Research: Space Physics*, 124, 4842–4851. <https://doi.org/10.1029/2019JA026744>





Received 20 MAR 2019

Accepted 20 MAY 2019

Accepted article online 31 MAY 2019

Published online 26 JUN 2019

Electron Density Retrieval From Truncated Radio Occultation GNSS Data

Haixia Lyu^{1,2} , Manuel Hernández-Pajares^{1,2} , Enric Monte-Moreno³ , and Estel Cardellach^{1,4} 

¹IEEC, Barcelona, Spain, ²UPC-IonSAT, Barcelona, Spain, ³UPC-TALP, Barcelona, Spain, ⁴ICE-CSIC, Barcelona, Spain

Abstract This paper summarizes the definition and validation of two complementary new strategies, to invert incomplete Global Navigation Satellite System Radio-Occultation (RO) ionospheric measurements, such as the ones to be provided by the future EUMETSAT Polar System Second Generation. It will provide RO measurements with impact parameter much below the Low Earth Orbiters' height (817 km): from 500 km down approximately. The first presented method to invert truncated RO data is denoted as Abel-VaryChap Hybrid modeling from topside Incomplete Global Navigation Satellite System RO data, based on simple First Principles, very precise, and well suited for postprocessing. And the second method is denoted as Simple Estimation of Electron density profiles from topside Incomplete RO data, is less precise, but yields very fast estimations, suitable for Near Real-Time determination. Both techniques will be described and assessed with a set of 546 representative COSMIC/FORMOSAT-3 ROs, with relative errors of 7% and 11% for Abel-VaryChap Hybrid modeling from topside Incomplete Global Navigation Satellite System RO data and Simple Estimation of Electron density profiles from topside Incomplete RO data, respectively, with 20 min and 15 s, respectively, of computational time per occultation in our Intel I7 PC.

1. Introduction

The increase of Global Navigation Satellite System (GNSS) Radio-Occultation (RO) measurements, such as Global Positioning System (GPS)/MET (Hernández-Pajares et al., 2000) CHAMP (Jakowski et al., 2002), COSMIC/FORMOSAT-3 (Olivares-Pulido et al., 2016), GRACE, EUMETSAT Polar System Second Generation (EPS-SG; ; Hernández-Pajares et al., 2017), PAZ (Cardellach et al., 2019), and FY3C/GNOS RO (Mao et al., 2016), has allowed for new developments in ionospheric sounding, disposing so far of the complete set of RO measurements, that is, those with negative elevations referred to the Low Earth Orbiters (LEO) horizon.

However, in this paper we deal with an initial limitation affecting some missions presently under preparation like EPS-SG: the lack of the topside part of RO observations. A related situation, but without the truncation of RO measurements, happens in the electron density reconstruction from RO data measured by lower altitude LEO, for example, CHAMP. To overcome the upper boundary problem, the inversion assisted by an adaptive electron density model of the topside ionosphere and plasmasphere was proposed (Jakowski et al., 2002). But the discontinuity at the transition height should be treated with care. While for truncated RO data, we have a double challenge: (1) the missing observations for a significant part of the RO measurements (more than 40% for EPS-SG) and (2) the longer length through the blind area makes the retrieval results more sensitive to the accuracy of the model. This last point has required the implementation of an still more realistic topside electron density model, the linear Vary-Chapman one, taking advantage of recent results. We showed in Hernández-Pajares et al. (2017) that once the electron density profile is well known below such ceiling height, for example, 500 km, it can be easily and accurately extrapolated. In this manuscript we will focus on the pending previous problem, that is, how to determine the electron density profile under such topside-truncated set of dual-frequency RO GNSS measurements, gathered from the LEO height, for example, approximately 800 km, paying attention to the accuracy but also to the computational load.

Indeed, the dual-frequency measurements provided by GNSS receivers onboard LEO in RO scenarios, with negative elevation angle, are very sensitive to vertical variability. This fact allows the retrieval of the electron density profiles below the LEO height. The new EPS-SG satellites at 817-km height are conceived for neutral atmospheric sounding. Nevertheless, this provides also opportunities for ionospheric sounding but with

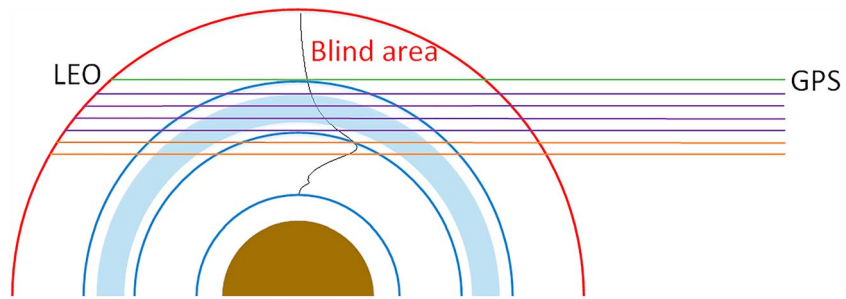


Figure 1. Layout of the incomplete radio-occultation measurements scenario studied in this work, showing up, as conceptual example, some transmitter-receiver rays illuminating three layers, in green, magenta, and orange colors. The height interval used to fit the Vary-Chap model is also represented (light blue color). LEO = Low Earth Orbiters; GPS = Global Positioning System.

RO measurements only taken with impact parameter height below 500 km (see layout in Figure 1). Some aspects of the electron density retrieval and impact on EPS-SG have been already studied, in particular a new electron density Vary-Chapman Extrapolation Technique (VCET) for impact parameters of 500 km up to the EPS-SG orbital height (Hernández-Pajares et al., 2017). This model can be considered an improvement of previous extrapolation approaches (e.g., Jakowski, 2005), which assumed a fixed scale height Chapman model for ionosphere in combination with an exponential model for plasmasphere. VCET is based on the predominant linear increase observed above hmF2 of scale height, due to its proportional dependence on temperature, as it was shown in Olivares-Pulido et al. (2016) and in the recent climatic models (Prol et al., 2018) that are based as well on top-sounding data (Prol et al., 2019). VCET assumes the availability of a properly estimated electron density profile.

Nevertheless, before applying such extrapolation, there is the need of an accurate estimate of the electron density profile below the first impact parameter height with measurements (500 km). In this regard we introduce two new techniques: the Abel-VaryChap Hybrid and the Simple Estimation of Electron density profiles, both modeling from topside Incomplete RO data (AVHIRO and SEEIRO, respectively). The two approaches do not depend on external models or data beyond the RO measurements. AVHIRO prioritizes the accuracy and SEEIRO prioritizes the estimation computing time in order to allow near real-time usage. The assessment of both techniques is presented with measurements of COSMIC/FORMOSAT-3 truncated up to 500 km, during four representative periods, by comparing the electron density profiles with the corresponding ones obtained from the full RO measurements.

The starting point for both approaches is the set of RO measurements gathered from the LEO, in our case the COSMIC/FORMOSAT-3 at a height of about $r_L = 800$ km. And they are truncated to a maximum impact parameter height equal to the expected value of $r_0 = 500$ km for EPS-SG. The dual-frequency ionospheric phase combinations, $L_I = L_1 - L_2$, are corrected by subtracting the Slant Total Electron Content (STEC) above the LEO orbit. These STEC values are computed from the Precise Orbit Determination antenna measurements, that is, with positive elevations, by means of a dual-layer tomographic voxel model which simultaneously estimate the electron density of the topside voxels and the carrier phase ambiguities, as described in Hernández-Pajares et al. (2017).

2. AVHIRO

The first method that we introduce in this paper is the hybrid approach—AVHIRO, which consists of Abel inversion and Vary-Chap model. It synergistically solves the full electron density, ambiguity term, and four parameters of Vary-Chap model at the same time, taking into account the nonlinear interactions between the unknown parameters. As it has been indicated above, Vary-Chap model summarizes the expected distribution of the topside electron density. And it is applied as constraint to improve the accuracy of the overall electron density estimation. Specifically, and following Figure 1, we can relate the ionospheric combination in length units, $L_I = L_1 - L_2$, where L_1 and L_2 are the carrier phases measured in frequencies f_1 and f_2 , with the known crossing lengths $l_{j,k}$ of the corresponding j th line-of-sight with each given k th layer and with the unknown electron density values N and carrier phase ambiguity in length units B_I . Following Hernández-Pajares et al. (2011), the small wind-up term is considered corrected and B_I contains the integer

terms in cycles, $\lambda_m N_m$, and instrumental phase delays for receiver and satellite, respectively, δb_m , $\delta b'_m$, and for frequencies $m = 1, 2$:

$$B_I = B_1 - B_2 = \lambda_1 N_1 - \lambda_2 N_2 + \delta b_1 - \delta b_2 + \delta b'_1 - \delta b'_2.$$

In this context we can express the ionospheric combination of carrier phases, from top to bottom, as

$$\begin{aligned} (L_I)_1 &= \alpha (2l_{1,1}N_1 + 2l_{1,2}N_2 + \dots + 2l_{1,x}N_x) + B_I \\ (L_I)_2 &= \alpha (2l_{2,1}N_1 + 2l_{2,2}N_2 + \dots + 2l_{2,x}N_x + 2l_{2,x+1}N_{x+1}) + B_I \\ (L_I)_3 &= \alpha (2l_{3,1}N_1 + 2l_{3,2}N_2 + \dots + 2l_{3,x}N_x + 2l_{3,x+1}N_{x+1}) + B_I \\ &\dots \\ (L_I)_6 &= \alpha (2l_{6,1}N_1 + 2l_{6,2}N_2 + \dots + 2l_{6,x}N_x + 2l_{6,x+1}N_{x+1} + 2l_{6,x+2}N_{x+2}) + B_I \\ &\dots \end{aligned} \quad (1)$$

The observation set of equation (1) can be summarized in matrix notation as $Ax = b$, where $x = (N_1, \dots, N_x, \dots, B_I)^T$ and $A_{j,k} = 2\alpha \cdot l_{j,k}$ for $k < M$ and $A_{j,M} = 1$ for the ambiguity coefficient, being $\alpha = 1.05 \times 10^{-17} \text{ m}^3$ the scaling factor converting electron content into delay (see Hernández-Pajares et al., 2011) and being M the number of unknowns.

From these equations, we cannot apply directly the Abel inversion algorithm (see, for instance, Hernández-Pajares et al., 2000), because the design matrix A is rank deficient due to the lack of observations above 500 km. In order to solve such rank-defect equations, the Vary-Chap model is added as constraint above 500 km, as it was indicated above, with parameters mainly estimated within the height range of 380 to 430 km. The Vary-Chap model is based on the physics of the problem as it has been mentioned above, allowing an extrapolation compatible with the observational data.

The Vary-Chap model is based on a nonlinear interaction between the parameters to be estimated. So in order to use it as prior, it is important to be aware of the difficulties related to the parameter estimation. The structure of the Vary-Chap model consists of two exponential terms of a variable z , as can be seen in equation (2). This variable z consists of terms that have to be estimated such as h_m and H . The estimation of these parameters by means of the conventional methods based on gradient search is difficult (Luenberger & Ye, 1984). This difficulty is due to the fact that small variations in the parameters give rise to very large changes in the value of the derivative, caused by the dependencies inside the exponential functions. These large changes are explained by the different scale of the values of the parameters and also by the nonlinear terms of the expression, which can be summarized as a multiplicative interaction between the parameters (i.e., N_m), the exponential of the inverse of a variable (i.e., $e^{\frac{1}{H}}$), and a double exponential of z .

A family of estimation methods that is robust to the problems of differentiability of the target function is the algorithms for minimization without derivatives. This family of algorithm searches for the optimum by comparing perturbations of a given candidate to the solution. The fact that instead of computing a derivative, they rely on comparisons, removing the problems related to the extreme variability of the derivatives, and the different scale of the unknowns. There are different algorithms in this family such as the Powell's method, the Nelder Mead algorithm, and the pattern search (see, for instance, Press et al., 1989). Due to the differences of scale of the parameters to be estimated, we selected the algorithm that in principle is more robust to this phenomenon, which is the Powell (1964) search method. This algorithm was used in order to estimate the electron densities below 380 km, the ambiguity term, and four Vary-Chap parameters, which are peak height h_m , peak electron density N_m , scale height at peak H_0 , and the derivative of scale height $\partial H / \partial h$, simultaneously. Afterward, the electron densities above 380 km are updated from the Vary-Chap model using the estimated parameters. The expression that relates the electron density N , with the height h , is the following:

$$N = N_m e^{\frac{1}{2}(1-z-e^{-z})}, \quad \text{where} \quad z = \frac{h - h_m}{H}, \quad (2)$$

$$H = \frac{\partial H}{\partial h}(h - h_m) + H_0, \quad (3)$$

where N and H represent the electron density and scale height at height h above peak, respectively.

The cost function of Powell search is mainly composed of two terms: one is $\|Ax - b\|^2$, and the other is the difference with respect to a reference estimate x_0 , weighted by λ which is a regularization parameter, $\lambda \|x - x_0\|^2$.

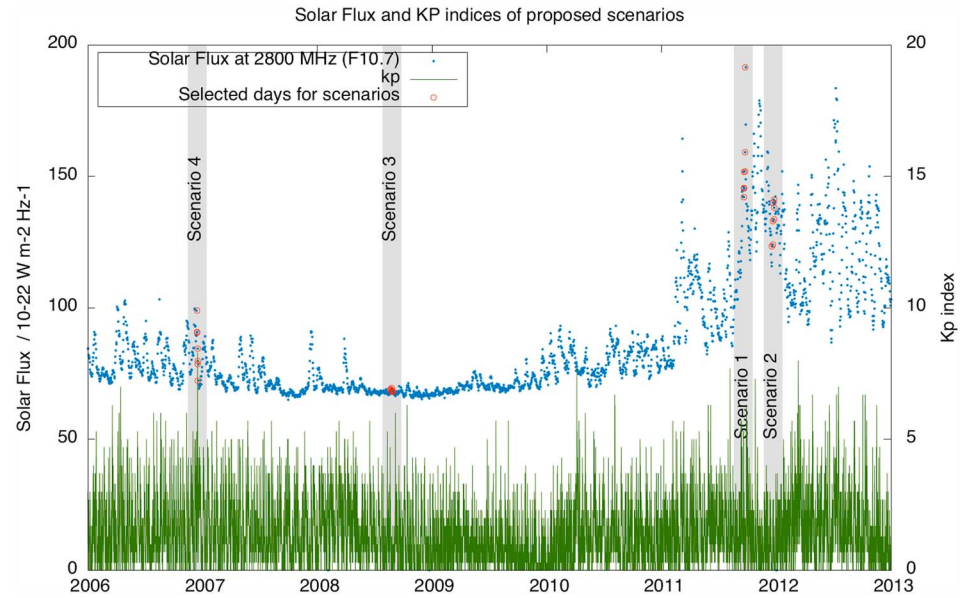


Figure 2. Solar flux and Kp index during the four selected periods, extracted from Hernández-Pajares et al. (2017).

The regularization parameter λ controls the smoothness of the estimation. Besides, additional penalization terms on h_m , N_m , H_0 , and $\partial H/\partial h$ are added to the cost function to constrain Vary-Chap parameters in a realistic range.

The unknown vector x in equation $Ax = b$ is composed of three parts, x^1 (electron densities from 380 and 1,000 km), x^2 (electron densities below 380 km), and x^{ambi} . The iterative algorithm for the estimation is described as follows:

1. Initial electron density profile below 500 km and ambiguity term are derived from Abel inversion, and then the full profile is extrapolated to 1,000 km. These values define the vector x_0 . Next we iterate updating this vector $x_0 = [x_0^1, x_0^2, x_0^{\text{ambi}}]$ each time, following next point.
2. The terms x_0^2 (current estimate of the electron densities below 380 km) and x_0^{ambi} are extracted from current unknowns x_0 , together with x_0^1 , which is calculated with the Vary-Chap model's parameters $[h_m, N_m, H_0, \partial H/\partial h]_0$. These parameters are initialized at the beginning with typical values: h_m and N_m are derived from the very first Abel inversion neglecting the electron content above 500 km, $H_0 = 30$ km and $\partial H/\partial h = 0.05$ from Olivares-Pulido et al. (2016). They form the x_{powell} .
3. The cost function of the Powell search is the sum of $\|Ax_{\text{powell}} - b\|^2$ and $\lambda \|x_{\text{powell}} - x_0\|^2$, where λ is obtained from the ratio of both estimated standard deviations in the previous iteration: the one from postfit residuals versus the one for peak electron density. And the Powell algorithm is applied in order to estimate an update of the values $[x^2, x^{\text{ambi}}, h_m, N_m, H_0, \partial H/\partial h]$.
4. The solution at the i th iteration x_{powell_i} can be computed by the searched vector $[x^2, x^{\text{ambi}}, h_m, N_m, H_0, \partial H/\partial h]_i$. Then we update x_0 by assigning x_{powell_i} to x_0 , and we go to step 2. Empirically, 10 iterations are performed in order to ensure the convergence of the algorithm.

3. SEEIRO

This is the second method that we introduce in this paper which, in contrast with the preceeding one, trades accuracy with speed. The SEEIRO algorithm iteratively estimates the electron density profiles under the assumption of an exponential behavior of the electron density among consecutive values in height. In this way, one variable scale height per topside height below 500 km can be easily obtained without the knowledge of h_m and N_m , and the Linear Vary-Chap model can be fitted from them and used for extrapolation and correcting the L_f observations for next iteration.

In the first iteration, $i = 0$, the system is initialized using only the Abel inversion of the available measurements below $r_0 = 500$ km and neglecting the electron density for higher altitudes, $r_0 < r < r_L$, and estimating

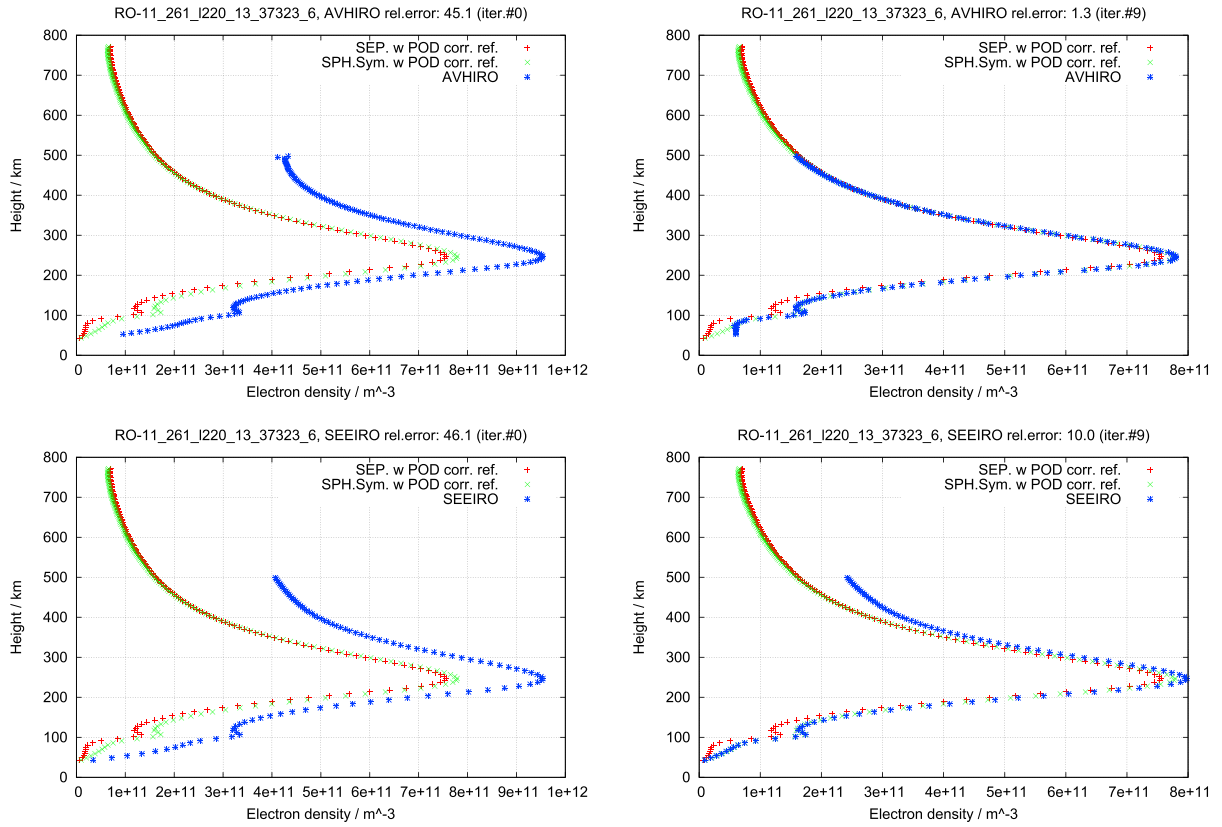


Figure 3. Example of the electron density (blue points) obtained from the measurements below 500 km of impact parameter height, with the AVHIRO (top row) and SEEIRO (bottom row) approaches, comparing the first and last iteration included in left- and right-hand columns, respectively. It corresponds to a single RO of satellite PRN13 with measurements from COSMIC/FORMOSAT-3 receiver L261 starting on second 37,323 of day 261 of year 2011. They are compared with two different solutions obtained from the complete set of measurements. The first one has been obtained by applying Abel inversion under the assumption of spherical Symmetry (green points) and the second one modeling the horizontal variability with the Separability concept mentioned above; the profile corresponding to hmF2 tangent point is represented with red points. In both reference cases, Precise Orbit Determination-data based Low Earth Orbiters topside corrections have been applied. RO = radio occultation; AVHIRO = Abel-VaryChap Hybrid density profile from topside Incomplete RO data; SEEIRO = Simple Estimation of Electron density profile from topside Incomplete RO data.

simultaneously the carrier phase ambiguity, B_i^0 , and the electron density $N_e^0(r_k)$, for $k = 1, \dots, M$, being M the number of layers defined with a width of Δr (e.g., $\Delta r = 3$ km).

In the subsequent iterations i , we focus now on the top values of the previous $(i - 1)$ solution, above the F_2 peak geocentric distance r_{mF2} and below the highest available geocentric distance r_0 and with a tolerance ϵ : $N_e^{(i-1)}(r_k)$ for $r_{mF2} + \epsilon \leq r \leq r_0 - \epsilon$. From these values, we estimate the scale height, assumed constant for each pair of consecutive values only. Indeed, we can approximate the Chapman function, equation (4), by the exponential approximation specially valid when $z \gg 1$:

$$N = N_m e^{\frac{1}{2}(1-z)}. \quad (4)$$

Then we can obtain the corresponding scale height values without the dependence on the F_2 peak height and density values, from two consecutive values:

$$H(r_k) \simeq \frac{-\Delta r}{2 \cdot \ln \frac{N_e^{(i-1)}(r_k)}{N_e^{(i-1)}(r_k - \Delta r)}}. \quad (5)$$

From the series of scale height values $H(r_k)$, the linear fit is performed following equation (3), removing iteratively outliers with residual greater than 2.5 times its standard deviation.

From the resulting linear model, the scale height is extrapolated, and a constant value H_0 is adopted when the estimated vertical gradient is not positive, that is, approximately in the 10% of cases. Afterward, the electron

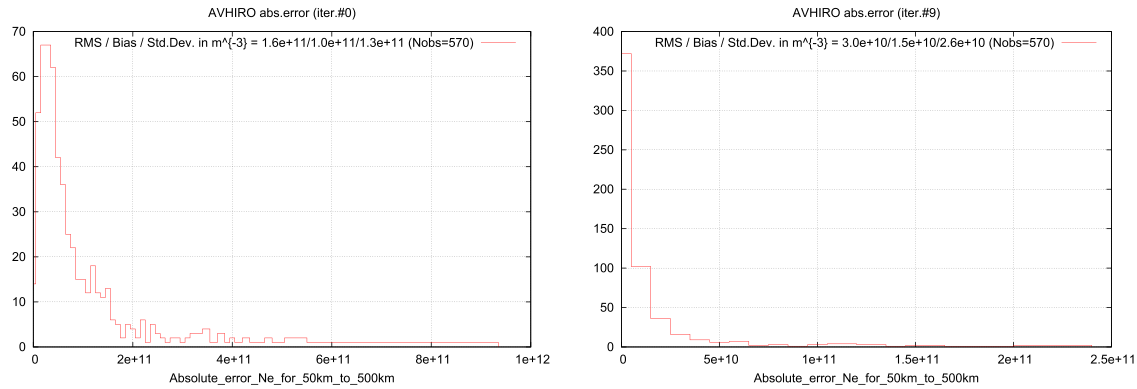


Figure 4. Histogram of the electron density error RMS values, one per occultation and expressed in per cubic meter. They correspond to the initial (left) and final (right) iteration of AVHIRO, for the selected COSMIC/FORMOSAT-3 radio occultations during days 346 of year 2006, 234 of year 2008, and days 261 and 352 of year 2011. AVHIRO = Abel-VaryChap Hybrid density profile from topside Incomplete RO data.

density is consistently obtained for $r > r_0$, with the exponential approximation equivalent to equation (5), that is,

$$N_e(r) = N_e(r - \Delta r) \cdot e^{-\frac{\Delta r}{2 \left[H_0 + \frac{\partial H}{\partial h} (h - h_m) \right]}}. \quad (6)$$

From these values, in the given iteration, the STEC between r_0 and r_L is mitigated within the measurements with impact factor below r_0 , and a new Abel inversion is performed repeating the same procedure described above, up to 10 times. This number of iterations is an optimal value empirically obtained, which ensures the convergence.

4. Estimation Assessment

In order to assess the performance of both AVHIRO and SEEIRO in the height range corresponding to the observations impact parameter heights (below 500 km), we have considered the selected set of 570 ROs corresponding to the first day of each one of the 4 weeks studied in Hernández-Pajares et al. (2017). They are representative of the previous solar cycle (see Figure 2).

One first illustrative example is shown in Figure 3. The performance of one typical occultation retrieval is compared between not applying (initial values) and applying these new techniques (last iteration). It can be seen that, in this case, the error goes down from 45–46% to 1.3% with AVHIRO and 10.0% with SEEIRO. We will see below that these final relative errors are not far from the most frequent ones.

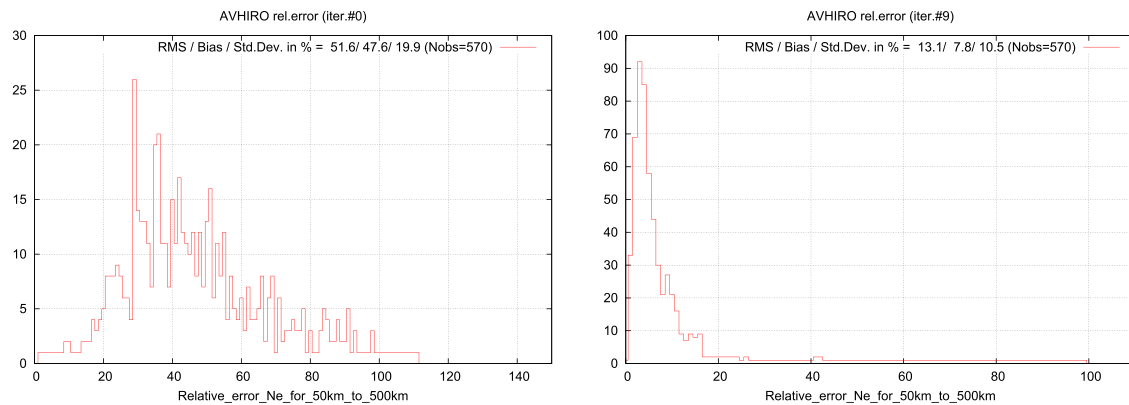


Figure 5. Histogram of the relative electron density error RMS values, one value per occultation and expressed in percent. They correspond to the initial (left) and final (right) iteration of AVHIRO, for the selected COSMIC/FORMOSAT-3 radio occultations during day 346 of year 2006, day 234 of year 2008, and days 261 and 352 of year 2011. AVHIRO = Abel-VaryChap Hybrid density profile from topside Incomplete RO data.

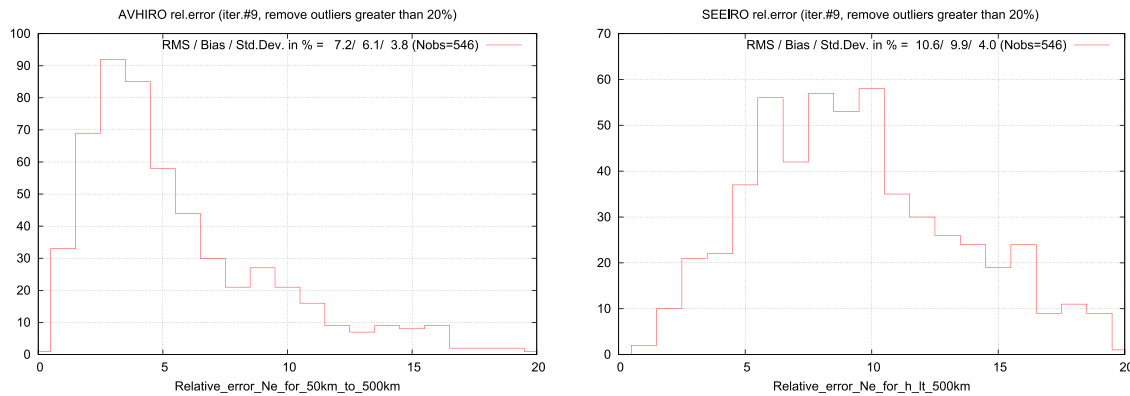


Figure 6. Histogram of the relative electron density error RMS values, one per occultation and expressed in percent, focused on the values smaller than 20%, the 96% of the analyzed radio occultations. They correspond to the final iterations of AVHIRO (left) and of SEEIRO (right), for the selected COSMIC/FORMOSAT-3 radio occultations during day 346 of year 2006, day 234 of year 2008, and days 261 and 352 of year 2011. AVHIRO = Abel-VaryChap Hybrid density profile from topside Incomplete RO data; SEEIRO = Simple Estimation of Electron density profile from topside Incomplete RO data.

We have considered the first day of each one of the four representative periods: namely, day 346 of year 2006 (low solar flux, before a major geomagnetic storm), day 234 of year 2008 (low to middle solar flux), and days 261 and 352 of year 2011 (high solar flux). The comparison of the absolute and relative Root Mean Square (RMS) error for AVHIRO are, respectively, shown in Figures 4 and 5. The error reduces from $1.0 \times 10^{11} \pm 1.3 \times 10^{11} \text{ m}^{-3}$ (51.6% of RMS) in the initial iteration to $1.5 \times 10^{10} \pm 2.6 \times 10^{10} \text{ m}^{-3}$ (13.1% of RMS) in the final one.

The histogram peak, that is, the mode of relative error, is 3% for AVHIRO versus 6–10% for SEEIRO (see Figure 6). Once we remove the values with relative error higher than 20% (23 of 570 ROs, i.e. the 4% of values), the relative error decreases to 7.2%, clearly below the corresponding value for SEEIRO: 10.6% (see again Figure 6). Nevertheless, SEEIRO is 70 times faster than AVHIRO, with an average processing time per RO in our Linux I7 PC of 15 s versus 20 min with AVHIRO.

These results strongly suggest that SEEIRO and AVHIRO techniques are appropriate, respectively, for near real-time and postprocessing determination of electron density profiles from topside-truncated RO data. A comparison of the main characteristics of both techniques is summarized in Table 1.

Table 1

Pros and Cons of AVHIRO Versus SEEIRO: Summary

	AVHIRO	SEEIRO
Ne relative accuracy	7%	11%
Predominant Ne rel. acc.	3%	6–10%
Ne absolute accuracy	$(1.5 \pm 2.6) \times 10^{10} \text{ m}^{-3}$	$(3.9 \pm 2.3) \times 10^{10} \text{ m}^{-3}$
Predominant Ne abs. acc.	$< 10^{10} \text{ m}^{-3}$	10^{10} m^{-3}
Calculation time per preprocessed RO	20 min	15 s
Suitable for NRT service?	Not now	Yes
Required ancillary information?	No	No
Required inputs	2-freq. GPS carrier phase meas., predicted GPS and LEO orbits (both)	
Convenient inputs	2-freq. GPS POD carrier phase meas. (both)	

Note. RO = radio occultation; AVHIRO = Abel-VaryChap Hybrid density profile from topside Incomplete RO data; SEEIRO = Simple Estimation of Electron density profile from topside Incomplete RO data; NRT = near real time; GPS = Global Positioning System; POD = Precise Orbit Determination; LEO = Low Earth Orbiters.

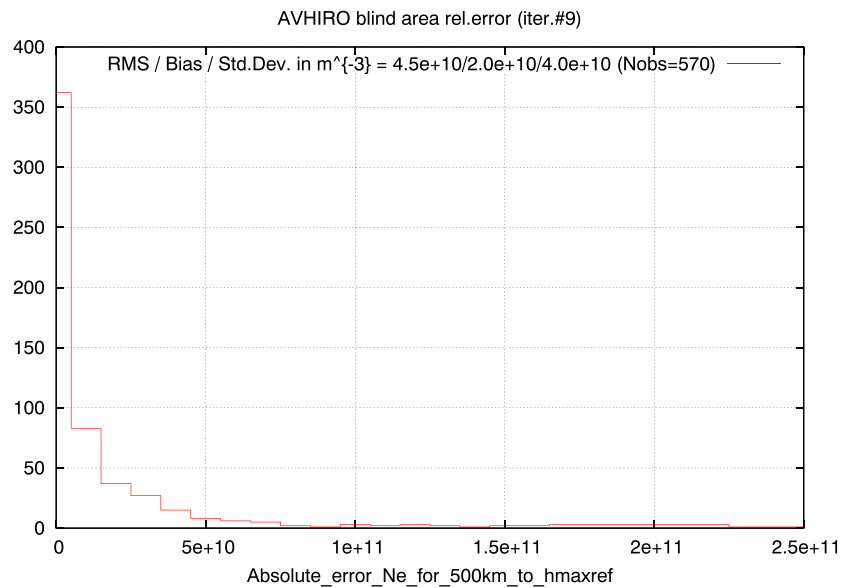


Figure 7. Histogram of the absolute topside electron density error RMS values, one value per occultation and expressed in per cubic meter. They correspond to the final iteration of AVHIRO, for the selected COSMIC/FORMOSAT-3 radio occultations during day 346 of year 2006, day 234 of year 2008, and days 261 and 352 of year 2011. AVHIRO = Abel-VaryChap Hybrid density profile from topside Incomplete RO data.

5. Extrapolation Assessment

Although the area below 500 km, tackled in previous section, is the main target of this work, the extrapolation precision for the topside part (above 500 km in this work) should be examined, since the electron densities in the blind area have a nonnegligible impact on the retrieval. In AVHIRO method, the full electron densities are estimated simultaneously, with a full linear Vary-Chap model for the topside part of the electron density profile, instead of by two steps to separate the observed and blind area. Hence, the topside

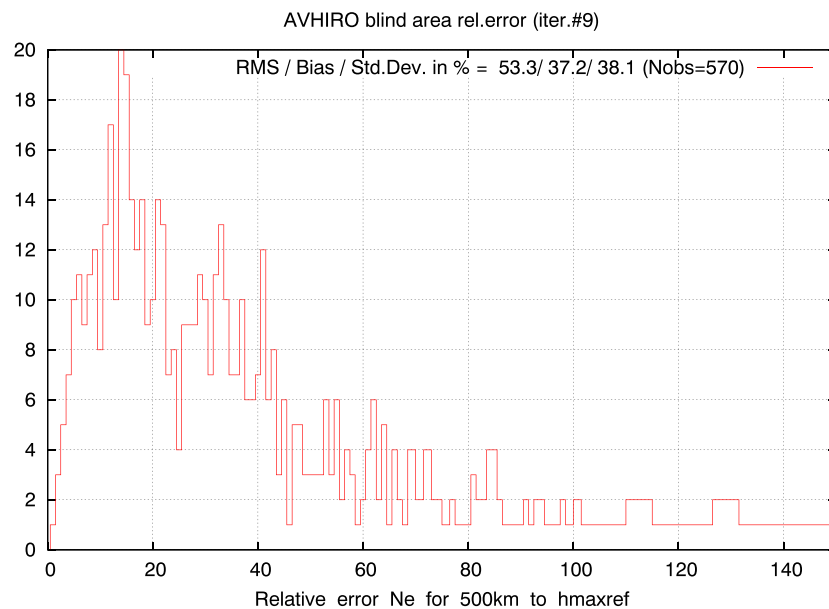


Figure 8. Histogram of the relative topside electron density error RMS values, one value per occultation and expressed in percent. They correspond to the final iteration of AVHIRO, for the selected COSMIC/FORMOSAT-3 radio occultations during day 346 of year 2006, day 234 of year 2008, and days 261 and 352 of year 2011. AVHIRO = Abel-VaryChap Hybrid density profile from topside Incomplete RO data.

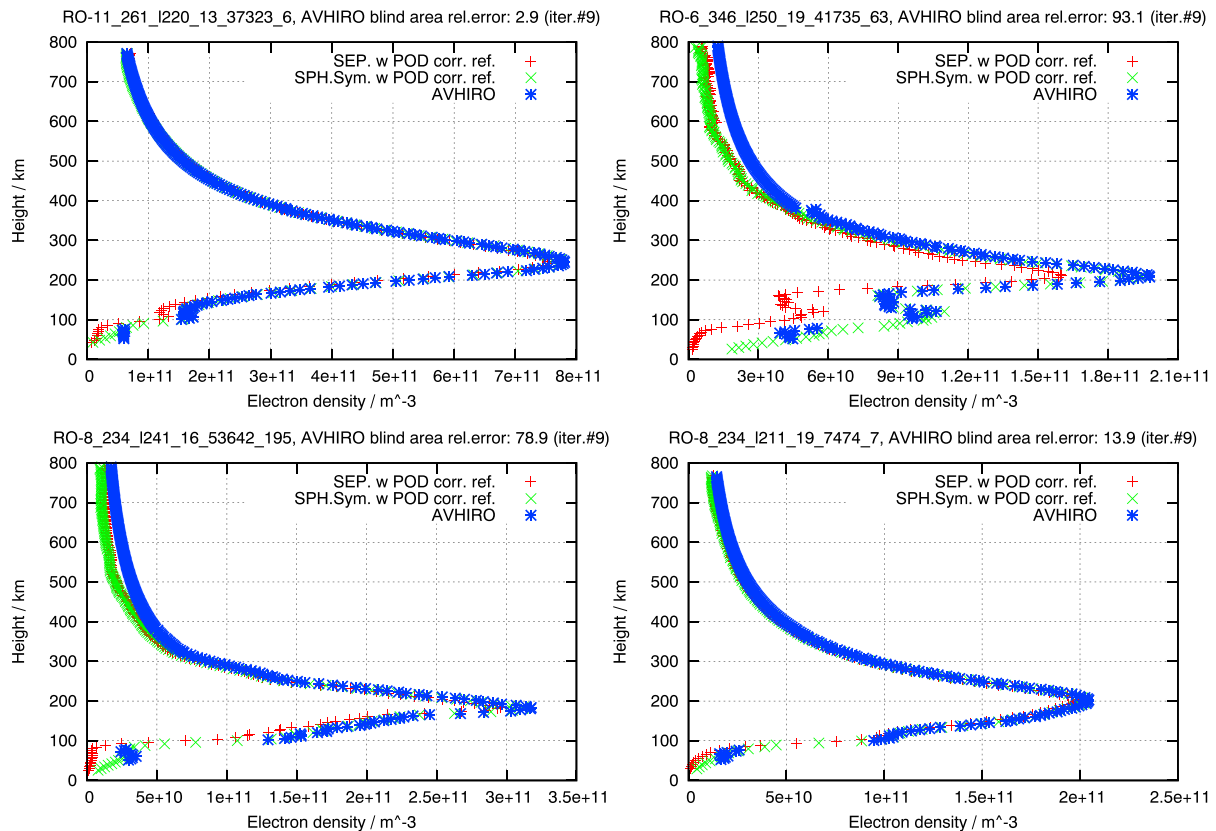


Figure 9. Four representative cases showing the Electron Density Profile (EDP) obtained with AVHIRO applied to the COSMIC/FORMOSAT-3 measurements below 500 km, compared with the EDP obtained from the full RO data set. RO = radio occultation; AVHIRO = Abel-VaryChap Hybrid density profile from topside Incomplete RO data; POD = Precise Orbit Determination.

assessment can to some extent reflect the performance of Vary-Chap model, which is shown in this section for completeness.

From absolute errors histogram (see Figure 7), the performance in the blind area is a little worse than but comparable to that in the area below 500 km, with bias $2.0 \times 10^{10} \text{ m}^{-3}$ and standard deviation $4.0 \times 10^{10} \text{ m}^{-3}$, which are in the same magnitude as those in the lower part. While the relative errors (see Figure 8) are quite large with 53.3% of RMS compared to 13.1% in the observed area. This can be easily explained by taking into account that the electron densities above 500 km are quite small and the sample number is limited for statistics, so the small absolute errors of electron density could produce big relative errors. For example, the four cases in Figure 9 show that, even with high relative error (93.1%), the extrapolation results by Vary-Chap model are very close to reference values, with $8.9 \times 10^9 \text{ m}^{-3}$ of absolute error inside error bars. Therefore, this proves good performance of Vary-Chap model in simultaneously extrapolating the topside electron density as well.

6. Conclusions

In this work we have presented a new Abel-VaryChap Hybrid modeling from topside Incomplete RO data (AVHIRO). This can complete the set of algorithms for ionospheric electron density retrieval from GPS RO data in EPS-SG with lack of measurements for impact parameter heights above 500 km, as a new postprocessing technique.

AVHIRO reduces, without the need of external data, the electron density error of the RO inversion with measurements up to 500 km regarding to the full inversion with observations up to 800 km: from 51.6% before to 13.1% percentage of electron density RMS after applying AVHIRO. In particular, it reduces the predominant relative error to 3% compared with the 6–10% obtained with the fast SEEIRO approach. Moreover, AVHIRO

provides simultaneously the linear Vary-Chapman extrapolated electron density profile with accuracies just slightly lower than those obtained at heights below 500 km with observations: $(2.0 \pm 4.0) \times 10^{10} \text{ m}^{-3}$ above versus $(1.5 \pm 2.6) \times 10^{10} \text{ m}^{-3}$ below 500 km.

Further potential improvements of the technique can be studied in future works, in particular to try to speed up AVHIRO to be hopefully suitable for near real time.

Acknowledgments

The authors are grateful to UCAR (United States) and NSPO (Taiwan) for providing the FORMOSAT-3/COSMIC RO data (<http://cdaac-www.cosmic.ucar.edu/>). The data used in this work are available online (ftp://chapman.upc.es/.AVHIRO_and_SEEIRO_results), or alternatively, it can be requested to Manuel Hernández-Pajares (manuel.hernandez@upc.edu). The activity has been supported by the Radio-Occultation Meteorology Satellite Application Facility (ROM SAF), which is a decentralized operational RO processing center under EUMETSAT. The work of the first author has been partially supported by the grant from the Chinese Scholarship Council.

References

- Cardellach, E., Oliveras, S., Rius, A., Tomás, S., Ao, C., Franklin, G., et al. (2019). Sensing heavy precipitation with GNSS polarimetric radio occultations. *Geophysical Research Letters*, 46, 1024–1031. <https://doi.org/10.1029/2018GL080412>
- Hernández-Pajares, M., Garcia-Fernández, M., Rius, A., Notarpietro, R., von Engeln, A., Olivares-Pulido, G., et al. (2017). Electron density extrapolation above F2 peak by the linear Vary-Chap model supporting new Global Navigation Satellite Systems-LEO occultation missions. *Journal of Geophysical Research: Space Physics*, 122, 9003–9014. <https://doi.org/10.1002/2017JA023876>
- Hernández-Pajares, M., Juan, J., & Sanz, J. (2000). Improving the Abel inversion by adding ground GPS data to LEO radio occultations in ionospheric sounding. *Geophysical Research Letters*, 27(16), 2473–2476.
- Hernández-Pajares, M., Juan, J. M., Sanz, J., Aragón-Ángel, A., García-Rigo, A., Salazar, D., & Escudero, M. (2011). The ionosphere: Effects, GPS modeling and the benefits for space geodetic techniques. *Journal of Geodesy*, 85(12), 887–907.
- Jakowski, N. (2005). Ionospheric GPS radio occultation measurements on board CHAMP. *GPS Solutions*, 9(2), 88–95.
- Jakowski, N., Wehrenpfennig, A., Heise, S., Reigber, C., Lühr, H., Grunwaldt, L., & Meehan, T. (2002). GPS radio occultation measurements of the ionosphere from CHAMP: Early results. *Geophysical Research Letters*, 29(10), 1457. <https://doi.org/10.1029/2001GL014364>
- Luenberger, D. G., & Ye, Y. (1984). *Linear and nonlinear programming* (Vol. 2). Switzerland: Springer.
- Mao, T., Sun, L., Yang, G., Yue, X., Yu, T., Huang, C., et al. (2016). First ionospheric radio-occultation measurements from GNSS occultation sounder on the Chinese Feng-Yun 3C satellite. *IEEE Transactions on Geoscience and Remote Sensing*, 54(9), 5044–5053.
- Olivares-Pulido, G., Hernández-Pajares, M., Aragón-Ángel, A., & García-Rigo, A. (2016). A linear scale height Chapman model supported by GNSS occultation measurements. *Journal of Geophysical Research: Space Physics*, 121, 7932–7940. <https://doi.org/10.1002/2016JA022337>
- Powell, M. J. (1964). An efficient method for finding the minimum of a function of several variables without calculating derivatives. *The Computer Journal*, 7(2), 155–162.
- Press, W. H., Flannery, B. P., Teukolsky, S. A., & Vetterling, W. T. (1989). *Numerical recipes*. Cambridge: Cambridge university press.
- Prol, F. d. S., Hernández-Pajares, M., Camargo, P. d. O., & Muella, M. T. d. A. H. (2018). Spatial and temporal features of the topside ionospheric electron density by a new model based on GPS radio occultation data. *Journal of Geophysical Research: Space Physics*, 123, 2104–2115. <https://doi.org/10.1002/2017JA024936>
- Prol, F. d. S., Themens, D. R., Hernández-Pajares, M., Camargo, P. d. O., & Muella, M. T. d. A. H. (2019). Linear Vary-Chap topside electron density model with topside sounder and radio-occultation data. *Surveys in Geophysics*, 40, 1–17. <https://doi.org/10.1007/s10712-019-09521-3>